Heriot-Watt University
Research Gateway

A Two-Port Multi-Polarization Rectenna with Orthogonal Hybrid Coupler for Simultaneous Wireless Information and Power Transfer (SWIPT)

Citation for published version:
Lu, P, Song, C & Huang, KM 2020, 'A Two-Port Multi-Polarization Rectenna with Orthogonal Hybrid Coupler for Simultaneous Wireless Information and Power Transfer (SWIPT)', *IEEE Transactions on Antennas and Propagation*, vol. 68, no. 10, pp. 6893-6905. https://doi.org/10.1109/TAP.2020.2993096

Digital Object Identifier (DOI):
10.1109/TAP.2020.2993096

Link:
Link to publication record in Heriot-Watt Research Portal

Document Version:
Peer reviewed version

Published In:
IEEE Transactions on Antennas and Propagation

Publisher Rights Statement:
© 2020 IEEE. Personal use of this material is permitted. Permission from IEEE must be obtained for all other uses, in any current or future media, including reprinting/republishing this material for advertising or promotional purposes, creating new collective works, for resale or redistribution to servers or lists, or reuse of any copyrighted component of this work in other works.

General rights
Copyright for the publications made accessible via Heriot-Watt Research Portal is retained by the author(s) and / or other copyright owners and it is a condition of accessing these publications that users recognise and abide by the legal requirements associated with these rights.

Take down policy
Heriot-Watt University has made every reasonable effort to ensure that the content in Heriot-Watt Research Portal complies with UK legislation. If you believe that the public display of this file breaches copyright please contact open.access@hw.ac.uk providing details, and we will remove access to the work immediately and investigate your claim.

Download date: 05. May. 2023

This article has been accepted for publication in a future issue of this journal, but has not been fully edited. Content may change prior to final publication. Citation information: DOI 10.1109/TAP.2020.2993096, IEEE Transactions on Antennas and Propagation

A Two-Port Multi-Polarization Rectenna with Orthogonal Hybrid Coupler for Simultaneous Wireless Information and Power Transfer (SWIPT)

Ping Lu, *Member IEEE,* Chaoyun Song, *Member IEEE*, and Ka Ma Huang, *Senior Member IEEE*

***Abstract*—A multi-polarization rectenna, consisting of a two-port antenna fed by an orthogonal hybrid coupler and a medium power rectifying circuit, is proposed. The orthogonal hybrid coupler has realized good isolation (S_{12} or S_{21} < -15 dB) between the two ports, which can be respectively connected to rectifying circuit and/or communication device for simultaneous wireless information and power transfer (SWIPT). Due to the symmetry of the coupler, the proposed rectenna can work at multi-polarization modes, i.e. the circular polarization for the single-port operation and the linear polarization for the dual-port operation. Besides, a medium-power rectifying circuit is proposed, where its maximum radio-frequency (RF)-to-direct current (DC) power conversion efficiencies is 53.6% (simulated) and 51.1% (experimental) at the input power of 0 dBm and 0.5 dBm, respectively. By using the coupler, the conversion efficiency and impedance matching of the rectenna can be significantly improved. In addition, the power division between the two ports is considered at different modes. Compared to other rectennas, the proposed multi-functional rectenna has merits of multiple polarizations and multi-mode, which can therefore be used for the incoming waves in arbitrary polarization for SWIPT and cope with the uncertainty in real-world communication environments.**

Index Terms—Multi-polarization, multi-functional rectenna, simultaneous wireless information and power transfer (SWIPT), two-port rectenna.

I. Introduction

With the rapid development of mobile communications, the demand for battery-free wireless devices is increasingly vigorous, especially from the standpoint to reduce the costs of battery replacements and disposal. For many difficult-to-wire communication devices (e.g., implantable devices, Internet of Things (IoT) sensors and monitors), using "wireless power" to charge the battery is necessary but also challenging. The rectenna, also named as "wireless battery", which can receive and convert free-space microwave power into direct current (DC) power, is supposed to wirelessly supply continuous power for the aforementioned portable devices at a distance [1]-[2]. The integration of rectennas and wireless communication device will enable brand-new technologies for wireless microwave power transmission (MPT) and data communication at the same time. Hence, the concept of Simultaneous Wireless Information and Power Transfer (SWIPT) was established, which has attracted significant attentions in developing the next generation mobile power network [3], [4].

Many rectennas have been introduced to the communication devices for MPT and data communication [5]-[10]. There are mainly two forms, i.e. one-port rectenna and two-port rectenna. For one-port systems, the antenna is not only used for wireless communications, but also used as an essential part of rectennas. However, such one-port rectenna can only receive power and transmit data by turns, rather than SWIPT [5]-[6]. Recently, some two-port rectennas for simultaneous power reception and data communication have been designed [7]-[8]. In [7], an aperture-coupled dual-polarization microstrip rectenna with high isolation between the two ports was designed for MPT and data communication. However, the reported rectenna had a complicated two-layer structure, and the operating frequencies of MPT and data communication were different, which limits the application scenarios. To achieve the aligned typical frequency band for MPT and data communication, a printed patch rectenna with a microstrip feed line and an alternative probe feed line was proposed for energy receiving and data communication. However, the isolation between these two ports was relatively low, only around 1.5 dB [8]. To improve the isolation at the same frequency band, a frequency reconfigurable rectenna that performs SWIPT was proposed [9]. By controlling the

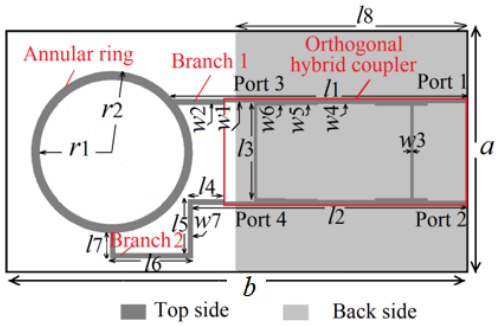

Fig. 1. Configuration of the reconfigurable receiving antenna. (The metal in dark gray is on the top side, and the partially ground in light gray is on the back side. (r_1 = 18.6 *mm*, r_2 = 17.8 *mm*, w_1 = 0.7 *mm*, w_2 = 1.27 *mm*, w_3 = 0.68 *mm*, w_4 = 1 *mm*, w_5 = 1.28 *mm*, w_6 = 1.44 *mm,* w_7= 1 *mm*, l_1= 69.46 *mm*, l_2= 55.46 *mm*, l_3=24.2 *mm*, l_4=8 *mm*, l_5=7.7 *mm*, l_6=24.4 *mm*, l_7= 1.27 *mm*, l_8= 52 *mm*, a=55 *mm*, b=105 *mm*.)

Manuscript received Sep. 30, 2019, revised Feb, 16, 2020, accepted Apr. 27. This work was in part by supported by National Natural Science Foundation of China (No. 51907130 and No. 61931009), the Postdoctoral Science Foundation of China (No.20504153007), and Sichuan Provincial Overseas Cooperation Grant (No. 2020YFH0091). (Corresponding author: Chaoyun Song)

P. Lu and K. M. Huang are with School of Electronics and Information Engineering, Sichuan University, Chengdu 610064, China and the Key Laboratory of Wireless Power Transmission Ministry of Education, Chengdu 610064, China. (e-mail: pinglu900424@scu.edu.cn)

C. Song is with the School of Engineering and Physical Sciences, Heriot-Watt University, Edinburgh EH14 4AS, Scotland, UK (e-mail: C. Song@hw.ac.uk).

0018-926X (c) 2020 IEEE. Personal use is permitted, but republication/redistribution requires IEEE permission. See http://www.ieee.org/publications_standards/publications/rights/index.html for more information.
Authorized licensed use limited to: Heriot-Watt University. Downloaded on June 15,2020 at 22:33:17 UTC from IEEE Xplore. Restrictions apply.

This article has been accepted for publication in a future issue of this journal, but has not been fully edited. Content may change prior to final publication. Citation information: DOI 10.1109/TAP.2020.2993096, IEEE Transactions on Antennas and Propagation

state of PIN switches, the proposed rectenna can be used to supply DC power for the electrical devices, and meanwhile support the data transmission function over the WLAN band and/or ISM band. However, additional loss was introduced by using such active switches, thereby decreasing the total output DC power. Besides, these proposed rectennas can only operate at linear polarization, which would cause a polarization mismatch loss [10].

To capture waves with multiple polarizations, some two-port circularly polarized antennas with an orthogonal hybrid coupler were designed [10]-[14]. Due to the aid of the coupler, two orthogonal signals with a 90° phase difference and a same magnitude are excited for releasing a circular polarization (CP). Besides, relatively high isolation between the two ports was observed. However, these circularly polarized antennas only used one of the two ports, which is a kind of waste for the additional ports.

In this paper, a multi-polarization rectenna with an orthogonal hybrid coupler is proposed for MPT and data communication. The proposed rectenna consists of a circular ring fed by the orthogonal hybrid coupler and a medium-power range (e.g., -10 to 10 dBm) rectifying circuit. Due to the symmetry of the coupler, the rectifying circuit and/or wireless communication devices can be connected to the receiving antenna for simultaneous/separate MPT and data communication with a well-supported right-handed circular polarization (RHCP), left-handed circular polarization (LHCP) and linearly-polarized (LP) operation. Besides, high isolation between the two ports at different polarization operations can be achieved. Owing to the coupler, the conversion efficiency of the rectenna can be improved when the impedance of the rectifying circuit is mismatched with that of antenna, since the reflected power can be returned back to the rectifying circuit for being reused. The proposed rectenna has great flexibility and a simple structure, and has merits of multi-functional, multi-polarization and multi-mode.

The rest of this paper is organized as follows. Section II focuses on the design of the two-port multi-polarization with the orthogonal hybrid coupler. Due to the reciprocity and symmetry of the coupler, the signal with same amplitude and 90° phase difference can be provided, and different modes, i.e. linearly-polarization (LP) and circularly-polarization (CP) can be achieved. Besides, the conversion efficiency of the rectenna can be improved as the input power and the output load varying. Section III shows the performance of the proposed rectenna, including the power distribution and active DC pattern. Results are compared with those reported two-port communication rectenna. Conclusions are drawn in Section IV.

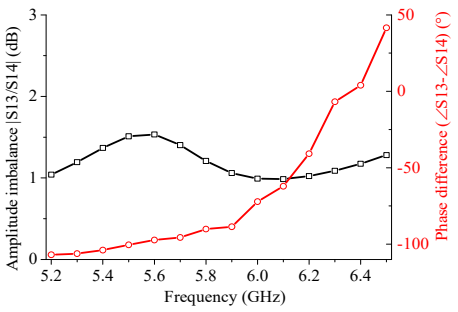

Fig. 2. Simulated performance of the proposed orthogonal hybrid coupler.

II. Two-Port Multi-Polarization Rectenna Design

The proposed multi-polarization rectenna contains a two-port receiving antenna and a medium-power rectifying circuit. An orthogonal hybrid coupler is introduced to connect the receiving antenna with the rectifying circuit. With a pair of 50Ω (SMA) coaxial connectors, any ports of the antenna can be flexibly connected to the rectifying circuit for MPT, and the other port can be used for data communication.

A. Two-Port Receiving Antenna Structure

The proposed receiving antenna, fabricated on a grounded Rogers4003C substrate (ε_r=3.38, $tan\delta$=0.0027) with a thickness of h=0.813 mm, is depicted in Fig. 1. A partially metallic ground ($l_8 \times a$) is printed on the back side of the substrate. The proposed antenna comprises an annular ring with the inner (outer) radius of r_1 (r_2) and a feeding network, which consists of a branch-line orthogonal hybrid coupler. The annular ring is connected to the coupler by two branches (Branch 1 and Branch 2). The dual branch is placed in the orthogonal direction, and is connected to the coupler with a 180-phase shift between its two output feed lines. Branch 1 is a straight feedline with the length of approximately $\lambda_g/4$, where λ_g is the guided wavelength. Branch 2 contains four-segment microstrip line with the total length of approximately $3\lambda_g/4$, and Branch 2 is bended for compact size. When the annular-ring antenna operates at the fundamental mode (TM_{11} mode), the ring size can be determined by the operating frequency f_0, that is,

$$\pi(r_1 + r_2) = \frac{c}{f_0\sqrt{\varepsilon_r}} \tag{1}$$

where c is the speed of light and ε_r is the effective permittivity. It can be seen that the wavelength at the operating frequency approximately corresponds to the mean circumference of the ring [15]. The widths w_2 (w_7) and w_1 of the microwave lines, connecting the ring and the coupler, determine their characteristic impedances of 50 Ω and 70 Ω, respectively. The final dimensions of the proposed receiving antenna with the coupler is listed below Fig. 1.

The hybrid coupler is constructed using rectangular loop-like strip line with four stubs that are configured as four ports.

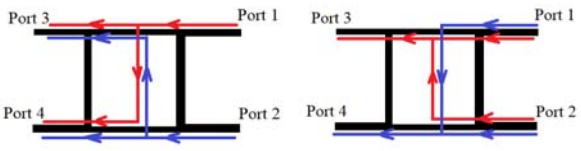

(a) (b)

Fig. 3. The signal (energy) transmission process at each port of the branch-line orthogonal hybrid coupler (The directions of the arrows can be reversible). (a) Separate Port 1 or Port 2 inputs (outputs) signal/energy. (b) Simultaneous Port 1 and Port 2 input (output) signal/energy.

0018-926X (c) 2020 IEEE. Personal use is permitted, but republication/redistribution requires IEEE permission. See http://www.ieee.org/publications_standards/publications/rights/index.html for more information.
Authorized licensed use limited to: Heriot-Watt University. Downloaded on June 15,2020 at 22:33:17 UTC from IEEE Xplore. Restrictions apply.

This article has been accepted for publication in a future issue of this journal, but has not been fully edited. Content may change prior to final publication. Citation information: DOI 10.1109/TAP.2020.2993096, IEEE Transactions on Antennas and Propagation

Two stubs (one of which is bended) on the left-hand side of the coupler (Port 3 and Port 4 in Fig. 1), are used to link the coupler with the circular ring antenna. The other two stubs on the right-hand side of the coupler are extended to form the two ports of the antenna, named Port 1 and Port 2.

With the orthogonal hybrid coupler, two signals with a 90° phase difference and an almost same magnitude are provided from Port 3 and Port 4. The simulated magnitude-imbalance (|S13/S14| in dB) and the phase-difference (∠S13-∠S14) at Port 1 are shown in Fig. 2. It can be seen that the bandwidth of 3dB magnitude imbalance covers the 5.2-6.5 GHz band, and the bandwidth of the 90°±10° (10° phase balance can achieve elliptic polarization at least) is over the 5.6-5.9 GHz band, containing 90° at 5.8GHz (ISM band). Due to the symmetrical structure of the coupler, assuming all the ports are well matched to the same coaxial connector, each port can be used to input or output the signal (energy), and the process of the signal (energy) transmission can be reversible, as shown in Fig 3. Hence, good performance of the hybrid coupler in the frequency band of 5.6-5.9 GHz ensures that the antenna can work at multi-polarization, i.e. left-hand/right-hand circularly-polarized mode (Mode 1) and linearly-polarized (LP) mode (Mode 2) in the corresponding frequency band, as listed below.

1) Mode 1: When only one of the ports (Port 1 or Port 2) feeds the antenna and the other is off, the receiving antenna operates at Mode 1. Due to the function of coupler, the input signal at Port 1(Port 2) is equally distributed to Port 3 and Port 4 with +(-)90° phase difference (see Fig. 3(a)), and then provides to the ring through one bended stub (Branch 2) and one straight short stub (Branch 1) with 180° phase difference, which are extended from Port 3 and Port 4, respectively. In this mode, the left-hand (right-hand) CP would be achieved.
2) Mode 2: When two ports (Port 1 and Port 2) are utilized to feed the antenna with +(-)90° sequential rotation. Due to the reciprocity of the coupler, the input signal from Port 1 and Port 2 is synthesized to output to the ring through Port 3 or Port 4, as displayed in Fig. 3(b). In this mode, the proposed antenna operates at the linear polarization (LP), and the two linear polarization directions are perpendicular to each other, named Mode 2.

The simulated and measured S-parameters of the antenna at the two modes are displayed in Fig. 4. It can be seen that the isolation between the two ports exceeds 15 dB in a frequency band of 5.7-5.83GHz, covering the operation frequency of 5.8 GHz (ISM band). Due to the high isolation, whether the antenna is fed by only one port (Mode 1) or two ports (Mode 2), S-parameter curves are the same at the two modes, i.e. the same operating frequency of LHCP, RHCP and LP. The antenna can work in a frequency band of 5.75-6.15 GHz/5.75-6.15 GHz at Port 1 or 5.7-5.85 GHz/5.7-5.85 GHz at Port 2 in the simulation/measurement. Obviously, a common band of 5.75-5.83 GHz (ISM band) can be achieved

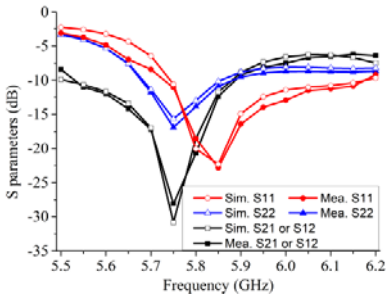

Fig. 4. Simulated and measured S-parameters at the two modes for LHCP, RHCP and LP.

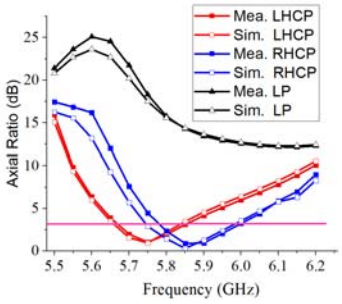

Fig. 5. Simulated and measured axial ratios (ARs) of the antenna at the two modes.

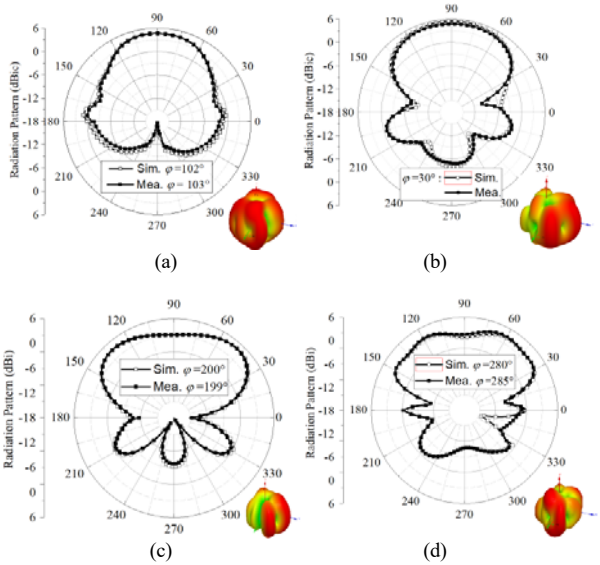

Fig. 6. Simulated and measured radiation pattern at 5.8 GHz. (a) Mode 1 fed by Port 1. (b) Mode 1 fed by Port 2. (c) Mode 2 fed by two ports with 90°. (d) Mode 2 fed by two ports with -90°.

for the two ports at the two modes, and the input impedances of the receiving antenna are (48.62–*j*0.43)Ω@5.8 GHz at Port 1 and (46.32-*j*0.73)Ω@5.8 GHz at Port 2, respectively. Due to ± 90° phase difference between the two ports, $|S_{11}|$ is slightly different from $|S_{22}|$ at the two modes, causing a small frequency deviation at the two ports (see Fig. 4).

Besides, the simulated and measured ARs of Port 1(Port 2) at the two modes are displayed in Fig. 5. It can be observed that the antenna fed by Port 1 achieves LHCP (AR<3) within

0018-926X (c) 2020 IEEE. Personal use is permitted, but republication/redistribution requires IEEE permission. See http://www.ieee.org/publications_standards/publications/rights/index.html for more information.
Authorized licensed use limited to: Heriot-Watt University. Downloaded on June 15,2020 at 22:33:17 UTC from IEEE Xplore. Restrictions apply.

This article has been accepted for publication in a future issue of this journal, but has not been fully edited. Content may change prior to final publication. Citation information: DOI 10.1109/TAP.2020.2993096, IEEE Transactions on Antennas and Propagation

5.7-5.85GHz/5.7-5.85GHz in the simulation/measurement. Having fed by Port 2, the RHCP (AR<3) frequency bandwidth covers from 5.75-6 GHz/5.77-5.98 GHz with a good agreement between simulated and measured results, which means that the antenna has achieved a good CP feature over the ISM 5.8 GHz band. While the two ports are excited simultaneously, the antenna works at the linear polarization (AR>10).

Also, the simulated and measured radiation patterns at the two modes in the direction of maximum gain are shown in Fig. 6. When the antenna is fed by using Port 1, the main beam with the simulated/measured maximum gain of 4.71/4.60 dBic is directed at (φ, θ) = (102°, 90°)/(103°, 90°), while fed by Port 2, the main beam with the maximum gain of 5.15/5.09 dBic is directed at (φ, θ) =(30°, 90°)/(30°, 90°). When the antenna is simultaneously fed by Port 1 and Port 2 with the sequential rotation of 90°, the main beam with the simulated/measured maximum gain of 4.97 dBi/4.92 dBi is directed at (φ, θ) =(200°, 50°)/(199°, 50°) , while with the sequential rotation of -90°, the main beam with the simulated/measured maximum gain of 4.42 dBi/4.16 dBi is directed at (φ, θ) =(280°, 60°)/(285°, 61°). Besides, the simulated (measured) antenna efficiencies η_a are 94.7% (93.8%) for using Port 1 solely, 96.8% (96.1%) for using Port 2 solely and 95.6% (94.9%) for using Port 1 and Port 2 simultaneously.

From the results, we can see the simulated and measured results coincide with each other very well for both Mode 1 and Mode 2. The S parameters of them are slightly different which might be induced by the antenna processing errors and the deviation of dielectric constant. For the decrease of the measured gain and antenna efficiency, it may be due to the loss of the SMA connector and the deviation of dielectric constant. As mentioned in the datasheet of the RO4003C substrate [16], the actual dielectric permittivity (ε_r) may increase from 3.38 to 3.55. By simulation, the maximum gain of the antenna drops by about 0.9 dB in these two modes. Besides, in the simulation, the loss of the SMA connector is not included. In general, the experimental measurement has validated the predicted performance of the proposed antenna.

B. Medium-Power Rectifying Circuit Design

In a typical domestic environment, the microwave power transmission with a high input power density is not allowed. Considering that, the power density (σ) should meet the safety standard, which is less than 1mW/cm^2 [17]. Hence, a medium-input power rectifying circuit is designed for the wireless power conversion at an optimal level. The layout of the rectifier is depicted in Fig. 7, where the proposed circuit layout is also printed on the top side of the grounded R04003C substrate.

The proposed rectifying circuit is composed of a pre-inductor, a series rectifier diode, a fan-shaped output filter and a matching circuit. To achieve high conversion efficiency under the condition of σ<1 mW/cm^2, the low-loss rectifying diode becomes a primary concern. Thus, a single HSMS 2850 Schottky diode with a low zero-bias junction capacitance (C_{j0} = 0.18 pF) and a low threshold voltage (V_{bi} = 0.35 V) is connected in series to the circuit [18]. Such diodes could consume relatively low power and offer a very fast switching speed at the frequency of interest (5.8 GHz).

An inductor (LQG15HH1N0S02) with some crossed microstrip stubs are used as an input matching filter to match the impedance at 5.8 GHz. The dimension of the stubs and value of inductors have been optimized (at the schematic level first and then full wave electromagnetic simulation) using the ADS software. A fan-shaped stub, which can replace the bypass capacitor without the need of vias, is used as an output filter. Having collaborated the output and input matching filters, the fan-shaped stub (output filter) can suppress high-order harmonics (by optimizing the radius and open angle of the fan-shaped stub in accordance with the higher-order harmonic frequencies at 11.6 GHz and 17.4 GHz), as well as smoothen the DC output voltage ripples. Furthermore, the matching circuit, including the input matching and the output matching circuit, are inserted between the antenna, the rectifier diode and the load, to achieve good impedance matching.

The rectenna is co-simulated by using HFSS (for antenna EM simulation) and ADS (for circuit nonlinear simulation) software. Considering that the operation frequency bandwidth of antenna ranges from 5.77 to 5.83 GHz at Mode 1(CP) and from 5.75 to 5.83 GHz at Mode 2 (LP), the rectifying circuit is proposed at a center frequency of 5.8 GHz with a relatively wide spectrum from 5.7 to 5.9 GHz. Due to the matching circuit, the input impedance of the rectifying circuit is (49.34+j0.57)Ω@5.8GHz at the input power of 0 dBm, which is conjugated-matched with that of the antenna at the two modes, therefore, good matching performance can be obtained at the desired operation frequency and input power.

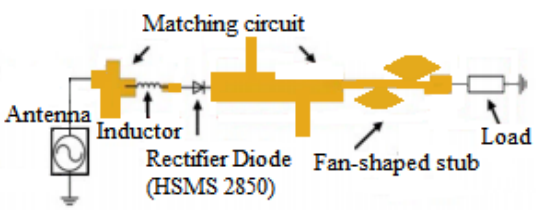

Fig. 7. Proposed rectifying circuit structure.

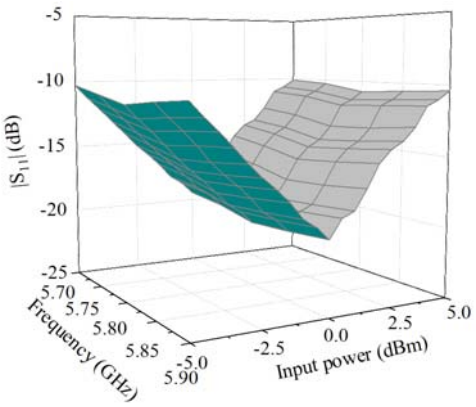

Fig. 8. Simulated S parameter of the proposed rectifying circuit versus frequency and input power.

0018-926X (c) 2020 IEEE. Personal use is permitted, but republication/redistribution requires IEEE permission. See http://www.ieee.org/publications_standards/publications/rights/index.html for more information.
Authorized licensed use limited to: Heriot-Watt University. Downloaded on June 15,2020 at 22:33:17 UTC from IEEE Xplore. Restrictions apply.

This article has been accepted for publication in a future issue of this journal, but has not been fully edited. Content may change prior to final publication. Citation information: DOI 10.1109/TAP.2020.2993096, IEEE Transactions on Antennas and Propagation

The simulated S-parameters of the rectifying circuit are displayed in Fig. 8. It can be seen that the rectifying circuit can work over a frequency band of 5.75-5.9 GHz under the input power range from -5 to 5dBm, where $|S_{11}|$<-10dB. Within these frequency bands and input powers, good matching between the antenna and rectifying circuit can be achieved, especially at 5.8 GHz and 0 dBm input power, the $|S_{11}|$ reaches the minimum value of -20.3 dB in this scenario.

Since the proposed receiving antenna has multi-polarization mode, the input impedance and the output power of the antenna (input impedance and input power of the rectifying circuit) would change at different modes, hence, the mismatch between the antenna and the rectifying circuit could exist in these scenarios. Due to the coupler, the RF-DC conversion efficiency can be improved for the mismatch (the input power and output load varying) [19]. As displayed in Fig. 9 (a), when the antenna operates at Mode 1, i.e. only one port is connected to the rectifying circuit and the other port is connected to a matched load. The rectifying circuit is implemented at Port 1 as an example, and it is replaced by a load with the complex impedance Z_{L1}. Assume that the loss of the coupler is ignored. When the impedance mismatch of the rectifying circuit exists, the reflected wave Γa_1 from Port 4 ($j\Gamma a_1$ from Port 3) re-transmits to Port 3 and Port 4 through the coupler, respectively, thus, we have the output wave b_3=-$j\Gamma a_1/\sqrt{2}$ (b_3=-$\Gamma a_1/\sqrt{2}$) at Port 3 and b_4=-$\Gamma a_1/\sqrt{2}$ (b_4=-$j\Gamma a_1/\sqrt{2}$) at Port 4, where Γ is the reflection coefficient at Port 1 or Port 2, and a_1 is the input wave at Port 1. Then, the reflected wave a_3=$j\Gamma\Gamma' a_1/\sqrt{2}$ (a_3=$\Gamma\Gamma' a_1/\sqrt{2}$) and a_4=$\Gamma\Gamma' a_1/\sqrt{2}$ (a_4=$j\Gamma\Gamma' a_1/\sqrt{2}$) are re-transmitted to the coupler and then delivered to Port 1 and Port 2 again, and the output wave b_1=0 (b_1=-$j\Gamma\Gamma' a_1$) and b_2=-$j\Gamma\Gamma' a_1$ (b_2=0), respectively, where Γ' is reflection coefficient at Port 3 or Port 4. For the reflected wave Γa_1, since Port 2 is well-matched and no wave is reflected from this port, the matching of Port 1 could still remain as b_1=0 after the first reflection, i.e. no reflected waves re-input to Port 1 (the unmatched port); While for the reflected wave $j\Gamma a_1$, no reflected waves output from Port 2 (matched port and b_2=0 after the first reflection), and the reflected wave b_1=-$j\Gamma\Gamma' a_1$ can be reused by the unmatched rectifying circuit. Hence, as the input power and the output load vary, either the impedance matching of the rectifying circuit could still be maintained after the first reflection with almost no reflected waves or the reflected wave can be reused to improve the overall conversion efficiency. The detailed information about the input power of the unmatched rectifying circuit can be found in subsections later (in Section III. A. Case 3)).

As displayed in Fig. 9 (b), at Mode 2, both the rectifying circuit and the communication device work with +90° sequential rotation as an example, and they are replaced by the loads with the complex impedance Z_{L1} and Z_{L2}. When both impedances of the rectifying circuit and communication circuit are mismatched, the reflected wave $j\Gamma a_1$ at Port 1 and Γa_1 at Port 2 will flow through the coupler and will be injected to ports 3 and 4, respectively. Thus, we have the output wave b_3=0 at Port 3 and $b_4 = \frac{}{\sqrt{2}} j\Gamma a_1$ at Port 4. Then, the output wave b_4 can be partially reflected and transmitted to the coupler. Therefore, we have the reflected wave a_4 =-$\frac{}{\sqrt{2}} j\Gamma\Gamma' a_1$, and the wave a_4 injection from Port 4 is delivered to Ports 1 and 2 through the coupler again. The output wave b_1 =$j\Gamma\Gamma' a_1$ at Port 1 and b_2 =$\Gamma\Gamma' a_1$ at Port 2 can be obtained, and the reflected wave a_1'=- $j\Gamma^2\Gamma' a_1$ and a_2'=-$\Gamma^2\Gamma' a_1$ can be recirculated back into the coupler. Due to the coupler, the power reflected from the communication device and rectifying circuit can be partially re-injected back to the rectifying circuit. Thus, the power can be reused and the RF-DC conversion efficiency can be improved.

The RF-DC conversion efficiency (η_r) of a rectifying circuit at a specified frequency can be calculated as follows,

$$\eta_r = \frac{V_{dc}^2 / Z_{Load}}{P_{in}} \times 100\% \quad (2)$$

where Z_{Load} is the load impedance, V_{dc} is the output DC voltage over the load, P_{in} is the input power of the rectifying circuit. According to (2), the simulated and measured RF-DC

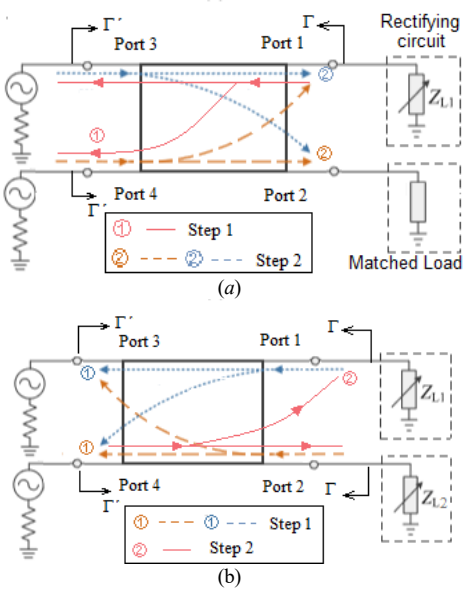

Fig. 9. Schematic diagram of the proposed rectifier with mismatching. (a) Only impedance of the rectifying circuit being mismatched. The reflected waves come from Port 3 or 4. (b) Both impedances of the rectifying circuit and communication circuit being mismatched.

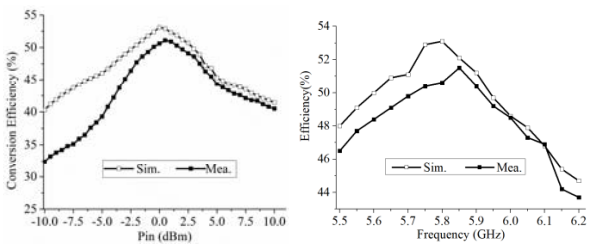

(a) (b)

Fig. 10. Simulated and measured RF-DC conversion efficiency η_r of the proposed rectifying circuit. (a) η_r *vs* input power at 5.8 GHz. (b) η_r *vs* frequency under the input power of 0 dBm.

0018-926X (c) 2020 IEEE. Personal use is permitted, but republication/redistribution requires IEEE permission. See http://www.ieee.org/publications_standards/publications/rights/index.html for more information.
Authorized licensed use limited to: Heriot-Watt University. Downloaded on June 15,2020 at 22:33:17 UTC from IEEE Xplore. Restrictions apply.

This article has been accepted for publication in a future issue of this journal, but has not been fully edited. Content may change prior to final publication. Citation information: DOI 10.1109/TAP.2020.2993096, IEEE Transactions on Antennas and Propagation

conversion efficiency η_r of the proposed rectifying circuit at 5.8 GHz with a 3000 Ω resistor is investigated, as shown in Fig. 10, where the input power varies from -10 to 10 dBm to meet the FCC (Federal Communications Commission) requirement for example. Under this condition, according to the equation of power density [20] ($\sigma=4\pi P_{in}/\lambda^2 G_r$, where λ is the wavelength in free space), the power density varying from 0.009 to 0.9 mW/cm^2 at 5.8 GHz, which is lower than the safety standard (σ<1mW/cm^2). Such an input power level could be satisfied in some applications at the frequency of interest, such as the Wireless Sensor Networks (WSN) and Radio Frequency Identification (RFID), in which the devices are located in the range from a few meters to tens of meters from the downtown RF sources (e.g. base station, cell tower, tag reader and sensor gateway) for testing environmental (air) quality and building quality. In addition, in the future mobile power network application, the mobile base station will be re-designed to transmit more power by using special modulated waves (e.g. chaotic signals and multi-sine signals [3], [4]), therefore the input power to the rectifier could be higher than that from the present communication systems, letting the proposed medium power rectifier under efficient operation. From Fig. 10(a), we can find that the simulated/measured conversion efficiency increases with the input power, and reaches its summit of 53.6%/51.1% at the input power of 0 dBm/0.5 dBm, and then decreases with the input power increasing further at 5.8GHz. Also, η_r with different frequency is shown in Fig. 10(b), where the simulated/measured conversion efficiency reaches the peak value of 53.6%/51.5% at 5.8 GHz/5.85GHz. As seen in the results below, the maximum conversion efficiency of 53.6% is achieved at 5.8GHz under the input power of 0 dBm, since the matching circuit is optimized under this condition. The measured maximum conversion efficiency is a little bit lower than the simulated one, and it appears at another input power or frequency. The discrepancy between the simulated and the measured results could be induced by the loss of the actual rectifier diode and SMA connector. Also, it may also come from the difference between ideal and realistic SPICE models of the components, such as the inductor and rectifier diode, which would lead to the mismatched and decrease the conversion efficiency. Furthermore, the actual rectifying diodes might not work in the effective operation mode when the input power is low, which resulted in a lower measured efficiency.

III. Performances of Multi-Function Rectenna

The fabricated rectenna is shown in Fig. 11, where the receiving antenna and the rectifying circuit were connected through SMA connectors and adapters with 50 Ω impedance. The experimental setup of the SWIPT system is displayed in Fig. 12, where the entire system was measured in the anechoic chamber. The signal source (modeled Agilent 83623L) was used to generate RF signal, and the RF power was magnified by an amplifier. Then, the amplified RF power was shunted by a Nadar 20 dB directional coupler. One way was fed to the transmitting dipole, while another way was fed to the power meter of Agilent E4416A to test the transmitting power. An omni-directional dipole antenna with calibrated gain of G_t was chosen as the transmitting antenna for the stable radiated power P_t in all directions [21]. The proposed rectenna with the gain of G_r was located at the distance L away from the transmitting antenna. Any ports of the antenna can be connected to the rectifying circuit for charging the low-power electronic device (e.g. LED), while the other port can be connected to a communication device (e.g., WiFi and Bluetooth wireless module with decoders) to realize the data communication. According to the incoming electromagnetic wave with different polarizations, the rectenna can effectively receive the power for MPT or/and data for communication, either separately or simultaneously. Presently there are no agreed (fixed) standards for SWIPT. Therefore, various schemes such as the time-splitting, power-splitting, frequency-aligned and frequency diverse SWIPT systems and examples have been proposed for the next generation mobile power network [4]. This work will mainly focus on the different cases in frequency-aligned and/or frequency diverse SWIPT by using power division at different operation modes.

A. Power Distribution Between Two Ports

Due to the symmetry and reciprocity of the coupler, through four ways of connection between the antenna, rectifying circuit and the communication device (see Fig. 3), the proposed rectenna can be flexibly switched to the optimal mode in accordance with the user's need.

Since the rectenna works at an identical frequency band or at different frequency bands for different ports and modes, the power division between the two ports should be considered. The input power P_{in} of the rectifying circuit, which is equivalent to the output power of antenna through the corresponding port, can be obtained according to the different modes of antenna, as displayed in following cases.

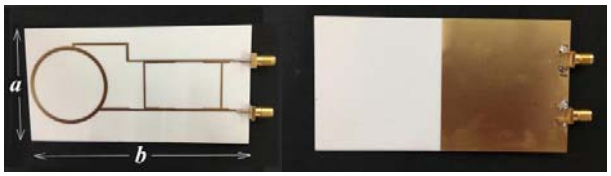

(a) (b)

(c)

Fig. 11. Fabricated proposed rectenna. (a) Top view of receiving antenna. (b) Back view of receiving antenna. (c) Medium power rectifying circuit. (a=55 mm, b= 105 mm, c1=7 mm, d1=25.1 mm.)

0018-926X (c) 2020 IEEE. Personal use is permitted, but republication/redistribution requires IEEE permission. See http://www.ieee.org/publications_standards/publications/rights/index.html for more information.
Authorized licensed use limited to: Heriot-Watt University. Downloaded on June 15,2020 at 22:33:17 UTC from IEEE Xplore. Restrictions apply.

This article has been accepted for publication in a future issue of this journal, but has not been fully edited. Content may change prior to final publication. Citation information: DOI 10.1109/TAP.2020.2993096, IEEE Transactions on Antennas and Propagation

1) Case 1: When the rectifying circuit or communication device is connected to Port *i* (*i*=1, 2) of the antenna and the other port is connected to a 50 Ω matched load, the antenna works at Mode 1. Within the operation frequency band of 5.77~5.83 GHz, the RF power with different polarizations can reach to the respective ports, and then flows to the rectifying circuit/the communication device. If the incoming waves are arbitrarily as well as linearly polarized, the polarization mismatch between the linear and circular polarization would be produced, and the received power is only 50% (3 dB loss) of the incoming wave (mismatch factor v=0.5). If the incoming waves are circularly polarized, the polarization matching is achieved, and the mismatch factor v=0. In this case, only Port *i* of the antenna can output the power/signal to the rectifying circuit/communication device. Due to the hybrid coupler, the port connected to 50 Ω matched load can be viewed as an isolated port, and no power is output to the 50 Ω load. Accordingly, all received RF power by the antenna is delivered to the rectifying circuit or communication device without the power division. Only the polarization matching is considered here. Then, the input power of the rectifying circuit $P_{in}(\theta, \varphi)$ at a given operation frequency (f) can be expressed by

$$P_{in}(\theta,\varphi,f) = (1\text{-}v)P_r(\theta,\varphi,f)\eta_a(f), \quad v = 0 \text{ or } 0.5 \qquad (3)$$

where $P_r(\theta, \varphi, f)$ and $P_{in}(\theta, \varphi, f)$ are the received power of the receiving antenna and the input power of the rectifying circuit, respectively, which are related to the incident angle (θ, φ) of the electromagnetic wave. $\eta_a(f)$ is the antenna efficiency which is also a function of frequency. Since only one port works, the proposed rectifying circuit or communication device will work independently, and the operating frequency of both can be identical or different, but it should be within the range of 5.77~5.83 GHz.

When the rectifying circuit is connected to Port *i* (*i*=1, 2) and the communication device is connected to the other port, the antenna operates at Mode 2, and both the rectifying circuit and the communication device work at the frequency bandwidth of 5.75~5.83GHz in the two orthogonal linearly polarizations. Hence, according to the incoming waves with different polarizations, the rectenna can receive the RF power in a specific polarization direction without polarization mismatch v=0, but with a maximum polarization loss v=0.5 in a circular polarization.

2) Case 2: When the proposed antenna operates at Mode 2, the rectifying circuit and the communication device at their respective ports will operate at the same frequency (f_0) simultaneously. The power division must be considered in this scenario. Assuming two ports are well matched to the same coaxial connector, the received power is equally output to the rectifying circuit and communication device (-3 dB at each port due to the hybrid coupler), and the power input to the rectifying circuit by Port 1 or Port 2 at the operating frequency (f_0) is written as follows.

$$P_{in}(\theta,\varphi,f_0) = \frac{1}{2}(1\text{-}v)P_r(\theta,\varphi,f_0)\eta_a(f_0), \quad v = 0 \sim 0.5 \qquad (4)$$

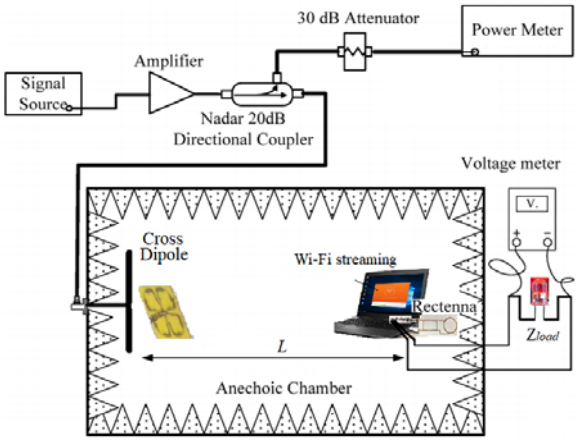

Fig. 12. Measurement setup. Scheme of the system with MPT and data communication. The data port is used for Wi-Fi streaming while the energy port is used to drive an LED. This is an illustrative example to demonstrate the multi-functionality of the proposed rectenna. The energy port can be utilized to charge the communication device itself with a power management unit (PMU) and an ultra-low-power DC-DC converter (model: BQ25504 from Texas Instrument) to boost and stabilize the output voltage (dependent on the power consumption and turn-on level of the device).

Note that due to the 90° phase difference between the two ports (Port 1 and Port 2) in this mode, the rectifying circuit and the communication device can work simultaneously rather than synchronously. Due to the power-splitting with asynchrony at Mode 2, the received power is equally split into two flows for data communication and power transmission at the same frequency [22]-[24].

3) Case 3: When the proposed antenna operates at Mode 2, the rectifying circuit and the communication device are both connected to the two ports simultaneously, but they work separately at different frequencies of f_i, (i=1,2) within the range of 5.75~5.83 GHz to reduce the crosstalk between the data communication and power transmission further. In this case, Port *i* can output the received power at the corresponding frequency of f_i to the rectifying circuit or communication device, and the other port can be equivalent to the connection of unmatched load at f_i, since the circuit or the device operates well at other operation frequency. As displayed in Fig. 13, a received RF wave at Port 3 (Port 4) is transmitted to Ports 1 and 2 through the coupler, and the

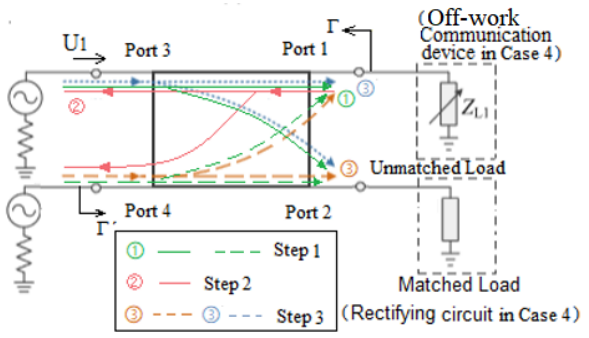

Fig. 13. Schematic diagram of the proposed rectifier with the unmatched port (the off-work communication device in Case 4) and matched port (rectifying circuit in Case 4).

0018-926X (c) 2020 IEEE. Personal use is permitted, but republication/redistribution requires IEEE permission. See http://www.ieee.org/publications_standards/publications/rights/index.html for more information.
Authorized licensed use limited to: Heriot-Watt University. Downloaded on June 15,2020 at 22:33:17 UTC from IEEE Xplore. Restrictions apply.

This article has been accepted for publication in a future issue of this journal, but has not been fully edited. Content may change prior to final publication. Citation information: DOI 10.1109/TAP.2020.2993096, IEEE Transactions on Antennas and Propagation

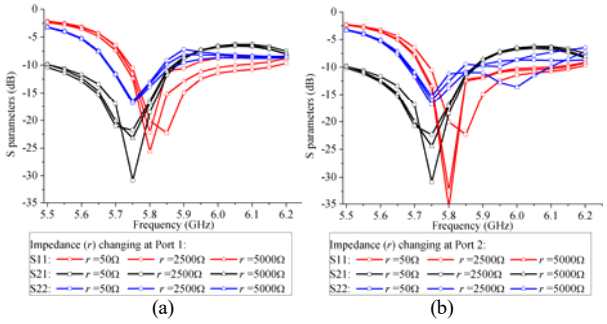

Fig. 14. S parameters of the antenna with different loading resistors (r) at Port 1 or 2. (a) Impedance of loading resistor (r) at Port 1 change. (b) Impedance of loading resistor (r) at Port 2 change.

reflected wave $a_1=j\Gamma U_1/\sqrt{2}$ ($a_1=\Gamma U_1/\sqrt{2}$) is generated at unmatched port, where Γ is the reflection coefficient at unmatched port, and U_1 is the incident input wave at Port 1. Due to high isolation of two ports, the matched port at f_i can still be well-matched (see Fig. 14), and no wave is reflected. Then, the reflected wave from the unmatched port transmits to Port 3 and Port 4 through the coupler, respectively, and the reflected waves at Port 3 or 4 are re-transmitted to the coupler and delivered to Port 1 and Port 2 again. Thus, the reflected wave $a_1'=-j\Gamma\Gamma^2U_1/\sqrt{2}$ ($a_1'=0$) is transmitted back to the antenna, and so forth. The detailed wave propagation process for an unmatched port can be referred to the analysis of Fig. 9(a). Due to the reflected waves, some power is attenuated by the unmatched port, but the reflected power can be recycled. Hence, the received RF power at f_i reaches to the two ports (unmatched port and matched port), and flows to the corresponding circuit or device. Then we have,

For the reflected wave $a_1=j\Gamma U_1/\sqrt{2}$ from the incident wave at Port 3,

$$P_{in}(\theta,\varphi,f_i)=\begin{cases}\frac{1}{2}(1-v)P_r(\theta,\varphi,f_i)\eta_a(f_i), & \text{for matched port}\\ \lim\limits_{n\to\infty}(1-|\Gamma|+|\Gamma|-\cdots+|\Gamma'|^{n-1}|\Gamma|^{n-1}-|\Gamma'|^{n-1}|\Gamma|^n)\cdot\frac{1}{2}(1-v)P_r(\theta,\varphi,f_i)\eta_a(f_i), & \text{for unmatched port}\end{cases} \tag{5}$$

For the reflected wave $a_1=\Gamma U_1/\sqrt{2}$ from the incident wave at Port 4,

$$P_{in}(\theta,\varphi,f_i)=\begin{cases}(1+|\Gamma'||\Gamma|)\cdot\frac{1}{2}(1-v)P_r(\theta,\varphi,f_i)\eta_a(f_i), & \text{for matched port}\\ (1-|\Gamma|)\cdot\frac{1}{2}(1-v)P_r(\theta,\varphi,f_i)\eta_a(f_i), & \text{for unmatched port}\end{cases} \tag{6}$$

where v=0~0.5, i=1,2, and n is the reflection number. Assume the reflected wave at Port 3 or Port 4 is totally reflected to the rectifying circuit rather than re-radiating by the antenna ($|\Gamma'|=1$). It can be seen that the input power at the two ports is relative to the reflection coefficient Γ at the mismatched port, where $\Gamma=\frac{Z_L-Z_0}{Z_L+Z_0}$, and Z_L is the impedance of the unmatched port and Z_0 is the characteristic impedance, $|\Gamma|<1$ [25]. Hence, (5) at unmatched port becomes,

$$\begin{aligned}P_{in}(\theta,\varphi,f_i)&=\lim_{n\to\infty}(1-|\Gamma|+|\Gamma|-\cdots-|\Gamma|^n)\cdot\frac{1}{2}(1-v)P_r(\theta,\varphi,f_i)\eta_a(f_i), \quad v=0\sim0.5,\ |\Gamma|<1\\ &=\lim_{n\to\infty}(1-|\Gamma|^n)\cdot\frac{1}{2}(1-v)P_r(\theta,\varphi,f_i)\eta_a(f_i), \quad v=0\sim0.5,\ |\Gamma|<1\\ &=\frac{1}{2}(1-v)P_r(\theta,\varphi,f_i)\eta_a(f_i), \quad v=0\sim0.5,\ |\Gamma|<1\end{aligned} \tag{7}$$

From (5)-(7), the reflected waves can be recycled due to the coupler, especially for the reflected wave $a_1=j\Gamma U_1/\sqrt{2}$ from the incident wave at Port 3, when the reflected wave at Port 3 or Port 4 is totally reflected to the rectifying circuit, or to the unmatched port. By numerous reflections, the maximum output power to the unmatched port can still reach to half, and the incident power of receiving antenna can be equally distributed to the matched port and unmatched port. With the frequency division multiplexing [7, 26-27], two independent channels at their respective frequencies can be achieved for SWIPT, and the incident power can be transmitted to the rectifying circuit and the communication device, respectively.

Above all, the proposed rectenna with the hybrid coupler can be used for SWIPT at the same frequency or at different frequencies, and the independent channel for data communication and power transmission can be built, due to high isolation between the two ports ($|S_{12}|$ or $|S_{21}|$<-15dB) and the power-splitting technology with independent operation in Case 1 or with asynchrony in Case 2 and frequency division multiplexing in Case 3.

4) Case 4: At Mode 2, if the communication device is turned off, the port impedance of the communication device is no longer 50 Ω, resulting in the impedance mismatch. But in this case, although the communication port is open circuit, the port impedance is not necessarily infinite. Due to the microprocessor chips and SMD circuit components on the communication circuit board, the port impedance is typically a large resistive value (3 to 30 kΩ, dependent on type of devices, and these devices could be resistive and subsequently produce a close circuit loop [28].), which can be measured directly using a multimeter. In our case, we assume the off-

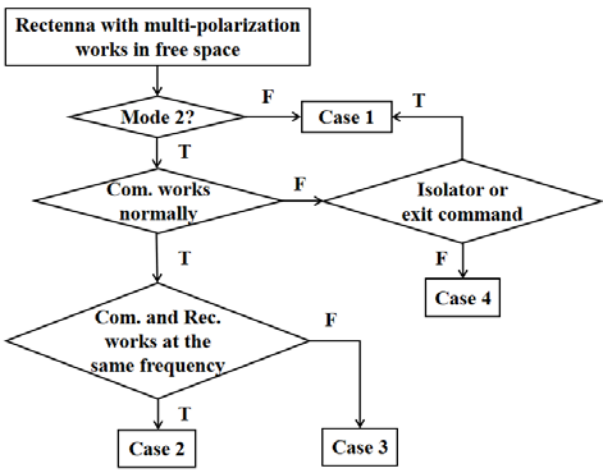

Fig. 15. Flow chart of the proposed rectenna with multi-polarization. (Com. represents communication device, and Rec. represents rectifying circuit.)

0018-926X (c) 2020 IEEE. Personal use is permitted, but republication/redistribution requires IEEE permission. See http://www.ieee.org/publications_standards/publications/rights/index.html for more information.
Authorized licensed use limited to: Heriot-Watt University. Downloaded on June 15,2020 at 22:33:17 UTC from IEEE Xplore. Restrictions apply.

This article has been accepted for publication in a future issue of this journal, but has not been fully edited. Content may change prior to final publication. Citation information: DOI 10.1109/TAP.2020.2993096, IEEE Transactions on Antennas and Propagation

mode impedance is up to 5000 Ω. Similar to Case 3 (for unmatched port), the unmatched port (Port 1) is connected to the off-work communication device, while the matched port (Port 2) is connected to the rectifying circuit, as displayed in Fig. 13. Due to the coupler, the rectifying circuit can still be well-matched with no reflected waves i.e. b_2=0 or some reflected waves can return to the rectifying circuit (b_2=ΓTU$_1$/$\sqrt{2}$). Hence, the power input to rectifying circuit at the operation frequency f is expressed by

$$P_{in}(\theta,\varphi,f)=\begin{cases}\frac{1}{2}\cdot(1-v)P_r(\theta,\varphi,f)\eta_a(f) \text{ for incident wave from Port 3,}\\ \frac{1}{2}\cdot(1+|\Gamma||\Gamma'|)(1-v)P_r(\theta,\varphi,f)\eta_a(f) \text{ for incident wave from Port 4,}\end{cases} \quad v=0\sim0.5 \tag{8}$$

Due to high isolation of the two ports, the rectifying circuit can still operate efficiently when the equivalent load (unmatched port) impedance of the communication device is varying. The impact of the loading resistor (r) variation at Port 1 or Port 2 has been investigated in Fig. 14. It can be seen that when r at Port 1 or 2 is increasing from 50 to 5000 Ω, the resonant frequency becomes slightly lower. But at the frequency of interest (5.75~5.83 GHz), the antenna can still work well at Mode 2 with one port being totally unmatched.

When the communication device is off-work, the device impedance can still be remained as 50 Ω matched load in the following two special situations: 1) The circuit of the communication device has an isolator; 2) A digital signal of exit command reaches to the communication device, but the device circuit does not change [9]. In these two situations, only the rectifying circuit works with the alternative port using a 50 Ω matched load, and the operation mode of rectenna is switched from Mode 2 to Mode 1, resulting in the operation of Case 1.

According to the different connections of the two ports to the rectifying circuit or/and the (off-work) communication device, the proposed rectenna can operate at different cases. The flow chart of working cases is summarized in Fig. 15.

B. Active DC Output Power Pattern

The output DC power (P_{dc}) of the rectenna with different incident wave directions can be expressed as

$$P_{dc}(\theta,\varphi)=P_{in}(\theta,\varphi)\eta_r(P_{in}) \tag{9}$$

where the incident wave arrives at the rectenna from the direction of (θ, φ). $\eta_r(P_{\text{in}})$ is the RF-to-DC conversion efficiency obtained by Eq. (2), which is related to P_{in}. Based on the analysis of the power division in different cases, the input power P_{in} of the rectifying circuit can be obtained by Eqs. (3)-(8), and the received power $P_r(\theta, \varphi)$ of the receiving antenna can be estimated by

$$P_r(\theta,\varphi)=\frac{P_tG_tG_r(\theta,\varphi)\lambda^2}{(4\pi)^2L^2} \tag{10}$$

For the multi-polarization scenario, the cross-dipole transmitting antenna is chosen in the measurement to achieve dual-linear polarization, which is perpendicular to each other [21]. The simulated and measured DC output power patterns in the above-mentioned Cases 1 and 2 at the same operation frequency f_0=5.8 GHz of the rectifying circuit and communication device are demonstrated as examples in Fig. 16, where the transmitting antenna with the radiated power P_t of 2 W (33 dBm) and a G_t of 2.15 dBi, and the distance (L) between the transmitting antenna and the rectenna is 0.25 m in the far field region (L>0.23m) for the maximum received power of 3.6 dBm. Whatever the power division is account for, the maximum conversion efficiency at the optimum input power of 0 dBm can be achieved.

In Case 1, the rectenna is connected to Port 1 or Port 2 flexibly, and the other port is connected to a 50Ω matched load. With the incident wave direction varying, the simulated (measured) DC output power of Port 1 varies from 0.003 mW(0.002 mW) to 0.89 mW(0.85 mW), and that of Port 2 varies from 0.005 mW(0.003 mW) to 0.98 mW(0.94 mW). Due to the higher gain obtained by Port 2, the DC power of Port 2 is higher than that of Port 1.

Similarly, in Case 2, the rectifying circuit and the communication device are connected to the two ports, and

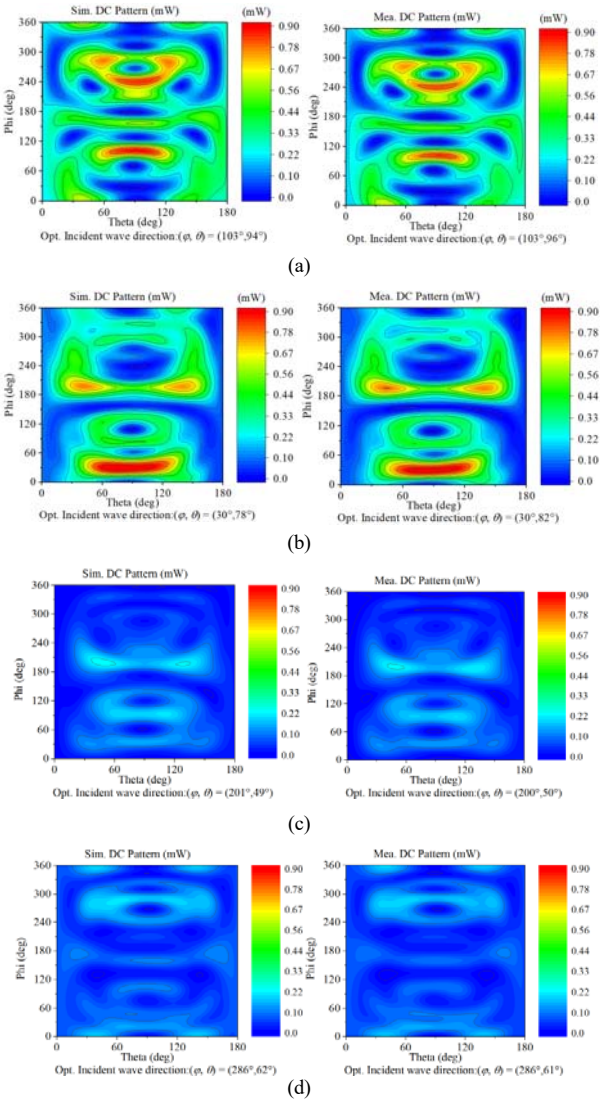

Fig. 16. Simulated and measured DC output patterns at 5.8 GHz for cross-dipole transmitting antenna with dual-linear polarization for example. (a) Case 1 fed by Port 1. (b) Case 1 fed by Port 2. (c) Case 2 fed by two ports with 90°. (d) Case 2 fed by two ports with -90°.

0018-926X (c) 2020 IEEE. Personal use is permitted, but republication/redistribution requires IEEE permission. See http://www.ieee.org/publications_standards/publications/rights/index.html for more information.
Authorized licensed use limited to: Heriot-Watt University. Downloaded on June 15,2020 at 22:33:17 UTC from IEEE Xplore. Restrictions apply.

This article has been accepted for publication in a future issue of this journal, but has not been fully edited. Content may change prior to final publication. Citation information: DOI 10.1109/TAP.2020.2993096, IEEE Transactions on Antennas and Propagation

TABLE I
COMPARISON OF TWO-PORT RECTENNAS WITH MPT AND DATA COMMUNICATION

Ref	Freq. (GHz)		S_{12} (dB)	Pol.	Input power (dBm)	Eff. (%)	Working mode	Size of rectenna (cm^2)
	Com.	MPT						
[7]	6.1	5.78	-25	LP	14	63	dividedly	9.2×3.8 (with two layers) (1.77λ×0.73λ@5.8GHz)
[8]	2.4		-1.5	LP	-	-	dividedly	6.76×2.76 (without rectifying circuit) (0.54λ×0.22λ@2.4GHz)
[9]	5.2/5.8		<-15	LP	5	50.2	Simultaneously or dividedly	8.9×9 (1.55λ×1.56λ@5.2GHz)
This work	LP:5.75-5.83 CP:5.77-5.83		<-15	LP, CP	0.5	51.1	Simultaneously or dividedly	13.01×5.5 (2.5λ×1.06λ@5.8GHz)

also the communication device works well. When the antenna is fed by Port 1 and Port 2 with the sequential rotation of 90°, as the incident wave direction varying, the simulated (measured) DC output power of Port 1 varies from 0.002 mW(0.002 mW) to 0.24 mW(0.23 mW), and the DC power of Port 2 is the same as that of Port 1, since the DC output power is halved by the two ports. With the sequential rotation of -90°, as the incident wave direction varying, the simulated (measured) DC output power of Port 1 or the Port 2 varies from 0.001 mW(0.001 mW) to 0.21 mW(0.20 mW). We can find that the DC output power in Case 2 is much lower than that in Case 1, since the received power is output to two ports simultaneously and the linear and dual-linear polarization is mismatched with v=0.5. Due to the power division and the polarization mismatch loss, P_{in} of both ports decrease, and η_r would decrease accordingly, then the DC output power in Case 2 would reduce further.

The simulated DC patterns basically coincide with the measured ones, except that the output power drops a little, and the optimum incident wave directions deviate slightly. The discrepancy between measurement and simulation may come from the actual loss of the rectifier diode. Due to packaging and fabricating, some parameters of these components may differ somewhat from those of simulation, which would cause the mismatching. Also, the additional loss of the actual SMA connector is not taken into account in the simulation, which would lead to a decrease in the actual output power.

C. Power Management Unit for System Integration

From Fig. 16, the instantaneous output DC voltage from the rectenna is too low to power directly a wireless device (WiFi, Bluetooth, etc.). To utilize the captured power of the proposed rectenna, a power management unit (PMU) with a DC-DC boost converter is required to meet the usable voltage level (e.g., 3.3V) for charging the communication device and drive the electronic circuit boards. In this design, an ultra-low-power DC-DC boost converter with a battery management (model: BQ25504 from Texas Instrument [30]) is employed as an example for demonstrating the full system integration of the proposed wireless powering system, as displayed in Fig. 17, where the minimum input voltage is down to 0.1 V and the DC-DC conversion efficiency maintains over 75% (up to 90%) for the input voltage range between 0.6 and 3V. Eventually, the output voltage could be programmed and regulated to a fixed level (e.g. 3.3V) for battery charging or direct driven of small electronics.

The output voltage of the rectenna with PMU versus the input power is given in Fig. 18, where the voltage input to the PMU is identical to the output voltage of the rectenna. It can be seen that the PMU starts to operate at the input power of -15 dBm with the output voltage of 0.16 V. The output voltage will be increased as a function of the input RF power whereas the amount of voltage boost is determined by the rectified DC power. Due to the utilization of DC-DC booster converter, the output voltage is substantially raised. More importantly, the selected PMU chipset (BQ25504) has a build-in function of MPPT (maximum power point tracking) to optimally charge a real-world device. For example, the output DC voltage with PMU reaches 1.5 V for battery charging at the input power of -3 dBm, where the output voltage without PMU is averaged about 0.82 V. When the output voltage of the rectenna without using PMC is 1.78 V, the PMU will reach its saturation level, which is 3.3 V at the input power of 3.5 dBm. With the input power increasing further, the steady DC output voltage of 3.3 V can be used for powering the communication device (WiFi, Bluetooth, etc.). By virtue of integrating the PMU and DC-DC model to the rectenna, the proposed system can be realistically used in read-world SWIPT applications. However, the end-to-end efficiency of WPT will not only be determined by our rectenna (as RX), it will also require advanced channel estimation and MIMO beamforming at the

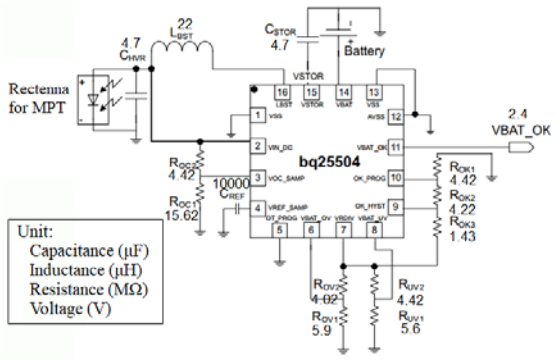

Fig. 17. Configuration of a BQ25504 power management unit with MPPT (maximum power point tracking) ultra-low-power DC-DC boost converter.

0018-926X (c) 2020 IEEE. Personal use is permitted, but republication/redistribution requires IEEE permission. See http://www.ieee.org/publications_standards/publications/rights/index.html for more information.
Authorized licensed use limited to: Heriot-Watt University. Downloaded on June 15,2020 at 22:33:17 UTC from IEEE Xplore. Restrictions apply.

This article has been accepted for publication in a future issue of this journal, but has not been fully edited. Content may change prior to final publication. Citation information: DOI 10.1109/TAP.2020.2993096, IEEE Transactions on Antennas and Propagation

base-station and gateway side, to maximize the spectral efficiency and overcome the channel fading. In this case, the overall SWIPT range and data-rate can be improved [31].

C. Discussion

The performance of the proposed rectenna for both MPT and communication is compared with some of the published two-port ones, as depicted in Table I. Obviously, the two-port rectenna given by [7] can achieve high conversion efficiency, but the published rectenna operates at high input power level and it works at two different frequency bands for MPT and data communication, respectively. Although the published rectenna [7] has a compact structure, it has a relatively complex structure using two layers, resulting in high antenna profile. For the common/aligned operation frequency band with low-profile structure, the reconfigurable rectenna is proposed [8]. However, due to the extra loss introduced by the switch, the conversion efficiency under the medium input power is low. In this design, with the implement of the coupler, the proposed rectenna can operate in the same frequency band at the common operation frequency or at different frequencies for MPT and/or data communication in different polarizations, and high isolation between the two ports ($|S_{21}|$ or $|S_{12}|$<-15dB) is achieved. Without the lossy switches, the proposed rectenna achieves higher conversion efficiency under the medium-power inputs than that in [9]. Although the size of our work is not compact, our design has achieved a reasonably small size with multiple working modes, which is comparable with that of the state-of-the-art SWIPT rectennas at the frequency of interest [9]. The proposed rectenna has a single-layer, simple and flexible structure, and the proposed rectenna can receive the electromagnetic waves at multi-polarization.

Due to the symmetric hybrid, the circular polarization and flexible structure can be realized for SWIPT at the expense of -3 dB division between the two ports. With the asymmetric hybrid [29], the power can be distributed to the rectifying circuit in any desired ratios for SWIPT, but the rectifying circuit and communication device may not be freely connected to the two ports for high signal to noise ratio (SNR) and high dc power. Besides, for the multi-polarization, i.e. RHCP, LHCP and LP, the advantage might go to our design with the symmetric hybrid, since the same magnitude (-3 dB division) can be provided from the two feeding ports for CP. Compared with some preliminary hardware demonstrations for SWIPT, our design has outstanding performance in terms of multi-working mode, reduced multipath polarization mismatch, multifunctionality and simple integration. The proposed design will be a very good example for realistic SWIPT in the future mobile power network applications.

IV. Conclusion

A two-port multi-polarization rectenna has been proposed for SWIPT. The proposed rectenna contained a two-port receiving antenna with orthogonal hybrid coupler and a medium-input-power rectifying circuit. By introducing an orthogonal hybrid coupler, the receiving antenna can work at multi-polarization, i.e. RHCP, LHCP and linear polarization, and high isolation between the two ports can be achieved. Besides, high conversion efficiency and excellent matching performance have been obtained at different modes although the output power and output impedance of the antenna could vary slightly at different modes. Due to the symmetry of the receiving antenna with the coupler, the communication device and/or the rectenna can be connected to any ports for MPT and data communication, either simultaneously or separately. The proposed rectenna can be used for these WSNs and RFIDs to receive multi-polarized RF waves for the desire of freely data communication and continuous power supplies anytime. The proposed rectenna could effectively resolve the polarization mismatch problem to enhance wireless communication and power quality. In addition, the design method of this rectenna can be further developed to cover dual-frequency multi-polarization rectennas (i.e. with the aid of a dual-band coupler [11]). This work has shown a relatively compact and efficient hardware development (with the system-level consideration of DC-DC conversion and power management unit) and demonstration for the SWIPT, which is of great significance to the future mobile power networks.

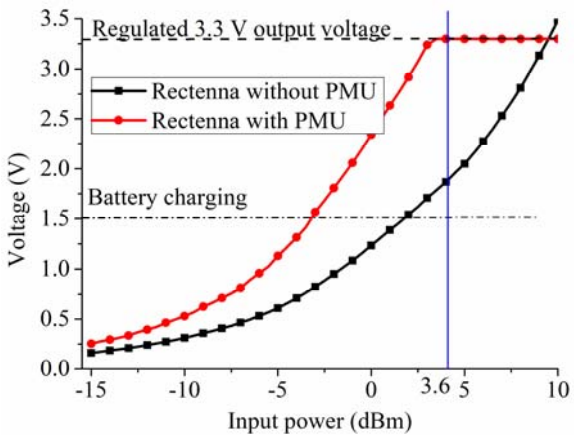

Fig. 18. Output voltage of the rectenna with PMU vs. input RF power to the rectifier. (The measured maximum received power is 3.6 dBm, where the steady output voltage can be regulated to 3.3 V for battery charging.)

References

[1] W. C. Brown, "An experimental low power density rectenna," in IEEE MTT-S Int. Microwave Symp. Dig., 1991, pp. 197–200.

[2] N. Shinohara, "Development of rectenna with wireless communication system," in Proc. 5th Eur. Conf. Antennas Propag. (EuCAP), 2011, pp. 3970–3973.

[3] T. D. Ponnimbaduge Perera, D. N. K. Jayakody, S. K. Sharma, S. Chatzinotas and J. Li, "Simultaneous wireless information and power transfer (SWIPT): recent advances and future challenges," in IEEE Communications Surveys & Tutorials, vol. 20, no. 1, pp. 264-302, Firstquarter 2018.

[4] B. Clerckx, A. Costanzo, A. Georgiadis and N. Borges Carvalho, "Toward 1G Mobile Power Networks: RF, Signal, and System Designs to Make Smart Objects Autonomous," in IEEE Microwave Magazine, vol. 19, no. 6, pp. 69-82, Sept.-Oct. 2018.

0018-926X (c) 2020 IEEE. Personal use is permitted, but republication/redistribution requires IEEE permission. See http://www.ieee.org/publications_standards/publications/rights/index.html for more information.
Authorized licensed use limited to: Heriot-Watt University. Downloaded on June 15,2020 at 22:33:17 UTC from IEEE Xplore. Restrictions apply.

This article has been accepted for publication in a future issue of this journal, but has not been fully edited. Content may change prior to final publication. Citation information: DOI 10.1109/TAP.2020.2993096, IEEE Transactions on Antennas and Propagation

[5] M. Ali, G. Yang, and R. Dougal, "A new circularly polarized rectenna for wireless power transmission and data communication," IEEE Antennas Wireless Propag. Lett., vol. 4, pp. 205–208, 2005.
[6] F.-J. Huang, C.-M. Lee, C.-L. Chang, L.-K. Chen, T.-C. Yo, and C.-H. Luo, "Rectenna application of miniaturized implantable antenna design for triple-band biotelemetry communication," IEEE Trans. Antennas Propag., vol. 59, no. 7, pp. 2646–2653, Jul. 2011.
[7] X.-X. Yang, C. Jiang, A. Z. Elsherbeni, F. Yang, and Y. Q. Wang, "A novel compact printed rectenna for data communication systems," IEEE Trans. Antennas Propag., vol. 61, no. 5, pp. 2532–2539, May 2013.
[8] R. Dehbashi, K. Forooraghi, and Z. Atlasbaf, "Dual-fed antenna for wireless power transmission and data communication," in Proc. IEEE Antennas Propag. Soc. Int. Symp., Jul. 2006, pp. 2201–2204.
[9] P. Lu, X.-S. Yang, and B. -Z. Wang, A two-channel frequency reconfigurable rectenna for microwave power transmission and data communication, IEEE Trans. Antennas Propag., vol. 65, no. 12, Dec. 2017, pp. 6976-6985.
[10] X．-M. Qing, Z. N. Chen, and H. L. Chung, Ultra-wideband circularly polarized wide-slot antenna fed by three stub hybrid coupler，2007 IEEE International Conference on Ultra-Wideband，pp.487-490, 2007.
[11] Y.-K. Jung and B. Lee, "Dual-band circularly polarized microstrip RFID reader antenna using metamaterial branch-line coupler", IEEE Trans. Antennas Propag., vol.60, no.2, pp. 786-791, Feb. 2012.
[12] K.-H. Lu, K.-C. Lin, and S.-K. Lin, Y.-C. Lin, "Wideband circularly-polarized aperture antenna arrays utilizing UWB directional coupler", Proceedings of the 2012 IEEE International Symposium on Antennas and Propagation, pp.1-4, July 2012.
[13] X. -M. Qing, Z. N. Chen, and H. L. Chung, "Ultra-wideband circularly polarized wide-slot antenna fed by three-stub hybrid coupler", 2007 IEEE International Conference on Ultra-Wideband, pp.487-490, Sept. 2007.
[14] X. -M. Qing, "Broadband aperture-coupled circularly polarized microstrip antenna fed by a three-stub hybrid coupler", Microwave and Optical Technology Letters, vol.40, no.1, Jan. 2004.
[15] Y. F. Lin, H. M. Chen, and S.C. Lin, "A new coupling mechanism for circularly polarized annular-ring patch antenna," IEEE Trans. Antennas Propag., vol.56, no.1, pp.11-16, Jan. 2008.
[16] RO4000 Series High Frequency Circuit Materials, Rogers Corp., Rogers, CT, USA, 2017.
[17] *OET Bulletin 65 Supplement C*. Accessed: Jan. 14, 2017. [Online].Available:http://www.Fcc.gov/Bureaus/Engineering_Technology/Documents/Bulletins/ort65.pdf
[18] HSMS 2850, Surface Mount RF Schottky Barried Diodes, Hewlett-Packard Technol., Palo Alto, CA, USA, 2017.
[19] M. Wei, Y. Chang, D. Wang, C. Tseng and R. Negra, "Balanced RF rectifier for energy recovery with minimized input impedance variation," in IEEE Transactions on Microwave Theory and Techniques, vol. 65, no. 5, pp. 1598-1604, May 2017.
[20] S. -D. Assimonis, S.-N. Daskalakis, and A. Bletsas, "Efficient RF harvesting for low-power input with low-cost lossy substrate rectenna grid," in Proc. IEEE RFID Technol. Appl. Conf. (REID-TA), Sep. 2014, pp. 1–6.
[21] C. Song, Y. Huang, J. F. Zhou, et al, "A high-efficiency broadband rectenna for ambient wireless energy harvesting," IEEE Transactions on Antennas and Propagation, vol. 63, no. 8, Aug. 2015.
[22] L. Krikidis, SWIPT in 3-D bipolar ad hoc networks with sectorized antennas, IEEE communications Letters, vol. 20, no. 6.
[23] J. Kim, B. Clerckx, and P. D. Mitcheson, "Signal and System Design for Wireless Power Transfer: Prototype, Experiment and Validation" arvix publication, Jan. 2019, pp.1-31. https://arxiv.org/pdf/1901.01156.pdf.
[24] J. Kim, B. Clerckx, and P. D. Mitcheson, "Prototyping and experimentation of a closed-loop wireless power transmission with channel acquisition and waveform optimization," in 2017 IEEE Wireless Power Transfer Conference (WPTC), May 2017, pp. 1–4.
[25] X. Y. Zhang, Z.-X. Du, and Q. Xue, High-efficiency broadband rectifier with wide ranges of input power and output load based on branch-line coupler, IEEE Transactions on Circuit and Systems-I: Regular papers, vol. 64, no. 3, Mar. 2017, pp.731-739.
[26] J. Wu, C.W. Zhao, Z.Y. Lin et al., "Wireless power and data transfer via a common inductive link using frequency division multiplexing", IEEE Trans on Industrial Electronics, vol. 62, no. 12, pp. 7810-7820, Dec. 2015.
[27] H. Kong, K. Feng, J. Wu, et al, "A novel conception of SWIPT System considering Information Independent Transmission," 2019 IEEE/CIC International Conference on Communications Workshops in China, pp. 200-203, 2019.
[28] C. Song, et al., "A Novel Quartz Clock with Integrated Wireless Energy Harvesting and Wireless Sensing for Smart Home Applications," IEEE Trans. Industrial Electronics., vol. 66, no. 5, pp. 4042 - 4053, Apr. 2019.
[29] H. -R. Ahn, I. Wolff, "Asymmetric four-port and branch-line hybrids," IEEE Transactions on Microwave Theory and Techniques, vol. 48, no. 9, 2000.
[30] BQ25504 Ultra Low Power Boost Converter with Battery Management for Energy Harvester, Technical datasheet, Texas Instrument, Jun. 2015.
[31] C. Boyer and S. Roy, "Backscatter communication and RFID: Coding, energy, and MIMO analysis," *IEEE Trans. Commun*., vol. 62, pp. 770-785, Mar. 2014.

0018-926X (c) 2020 IEEE. Personal use is permitted, but republication/redistribution requires IEEE permission. See http://www.ieee.org/publications_standards/publications/rights/index.html for more information.
Authorized licensed use limited to: Heriot-Watt University. Downloaded on June 15,2020 at 22:33:17 UTC from IEEE Xplore. Restrictions apply.